NSF/RA-760837

CYCLIC SHEAR BEHAVIOR OF R/C PLASTIC HINGES

by

Shao-Yeh M. Ma
Bechtel International

Egor P. Popov
Vitelmo V. Bertero
Department of Civil Engineering
University of California, Berkeley

INTRODUCTION

For medium-rise reinforced concrete (R/C) buildings, ductile moment-resisting space frames (DMRSF) are frequently used in design as lateral force-resisting structural systems. In order to prevent failure of such buildings during strong shaking, reliance is generally placed upon rigidity in the elastic range of the R/C frame components, and upon the capacity of these components to absorb and dissipate the energy fed into the structures from earthquake motions through large inelastic deformations. The inelastic deformations are usually developed at certain critical regions in the frame. These critical regions, usually called plastic hinges, are located at points of maximum internal forces. In DMRSF it is common practice to force the development of these critical regions at ends of the girder close to column connections where inelastic behavior is the result of either bending alone or bending and shear (Fig. 1). To determine the hysteretic behavior of such regions under earthquake-like excitations, numerous experimental investigations have been conducted in the past [1-6]. Most of these investigations have shown that under repeated cycles of load reversals, as the number of cycles increases, a progressive degradation in the force-deformation relationships of these regions occurs. These phenomena resulting in pinched hysteretic loops, usually lead not only to significant reduction in the energy dissipation per cycle of these regions, but may also lead to failure.

The larger the shear forces acting in these regions, the larger the observed degradations. Although the importance of shear reversals in controlling the hysteretic behavior of such regions has been pointed out in the past [1], no comprehensive study has been made to determine experimentally the mechanism for observed degradations. Therefore, a clear understanding of such hysteretic behavior has not yet been achieved.

The authors have carried out a series of studies on the hysteretic behavior of R/C flexural critical regions subjected to different levels of shear forces [4-8]. In these studies, the shear force-shear distortion responses were obtained for beams with different spans, reinforcement, and section shape as well as under different loading histories. In most of these studies, measurements of deformations of the critical regions undergoing inelastic load reversals have been

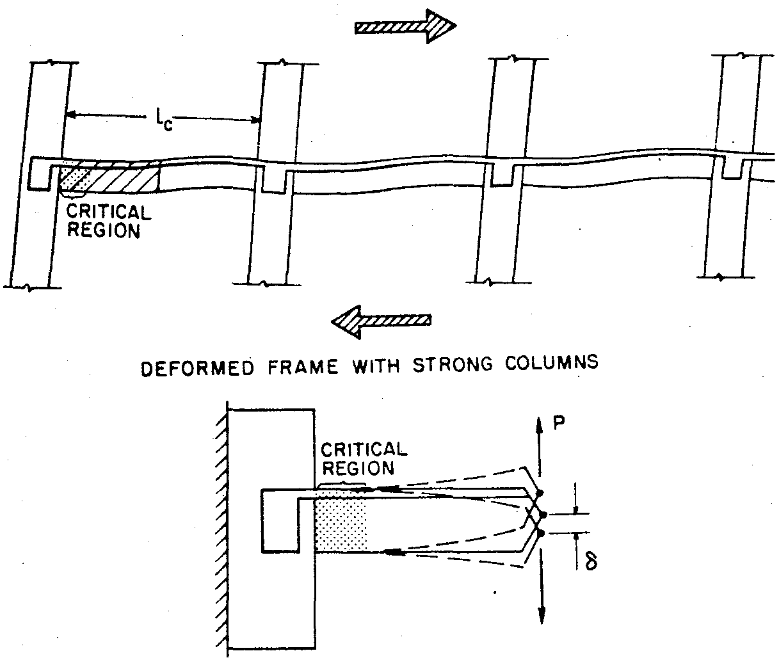

Fig. 1 Selected Test Specimen

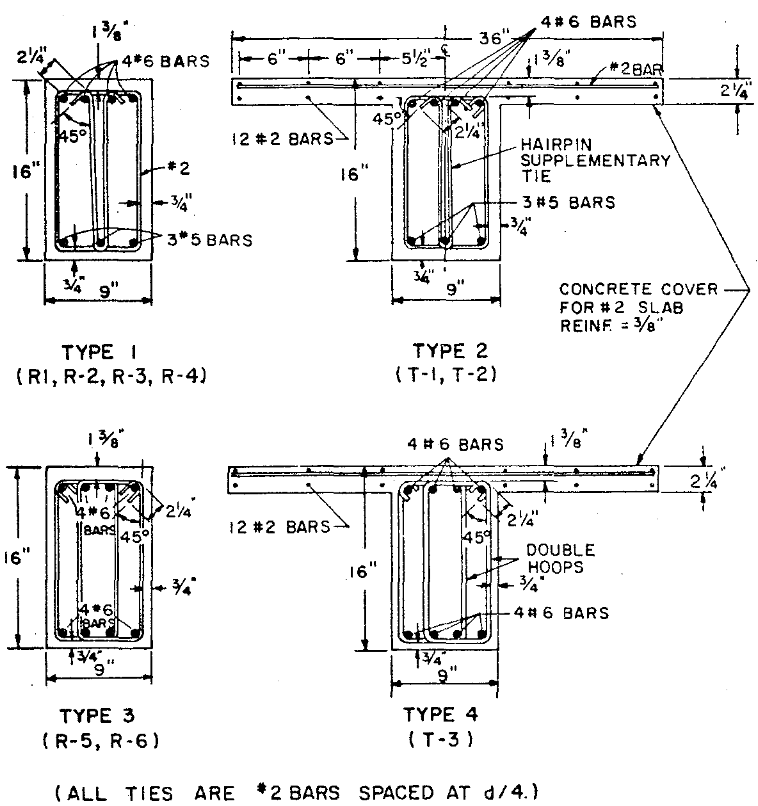

Fig. 2 Beam Section Details

conducted using different techniques with extensive instrumentation in order to study in detail the nature of shear distortion occurring in the regions.

Objectives and Scope. - With the data available from the studies conducted by the authors and others, it is possible to attempt to define the actual mechanisms of degradation in stiffness, strength and energy capacities that have been observed in the critical regions under earthquake-like excitations. The main objective of this paper is to present the results of such an attempt.

The main data analyzed were obtained from tests on nine cantilever beams. After a brief description of the test specimens and test procedures, the general behavior of the beams is discussed, with emphasis on the failure mechanism and how it is modified under different amounts of shear. Conclusions regarding the observed behavior are drawn, and their implications in aseismic design of ductile resisting frames are discussed.

TEST SPECIMENS, EXPERIMENTAL SET-UP AND LOADING PROGRAM

Test Specimens. - The data analyzed herein were obtained in a series of tests on nine half-size (9 in. x 16 in. rectangular cross-section) cantilever beams [8]. The parameters investigated were: section shapes (rectangular or tee shape, Fig. 2), amount of bottom reinforcement, amount of web reinforcement, shear span length, and loading history. The dimensions of these beams represent one-half scale models of a 20-story R/C office building.

SPECIMEN PROPERTIES

SPECIMEN	ℓ/d (in./in.)	ρ	ρ'	ρ_b	Top* Reinf. (bars)	Bot.** Reinf. (bars)	Stirrup*** Tie (bars)	Tie Spacings (in.)	ρ''	f'_c (Ksi)	f_r (Psi)
BEAM R-1	4.5	.014	.0074	.030	4#6	3#5	#2	3.5	.0053	5.07	510
BEAM R-2	4.5	.014	.0074	.026	4#6	3#5	#2	3.5	.0053	4.19	455
BEAM R-3	4.5	.014	.0074	.028	4#6	3#5	#2	3.5	.0100	4.58	475
BEAM R-4	4.5	.014	.0074	.027	4#6	3#5	#2	3.5	.0100	4.38	460
BEAM R-5	2.8	.014	.0140	.028	4#6	4#6	#2	3.5	.0100	4.58	480
BEAM R-6	4.5	.014	.0140	.027	4#6	4#6	#2	3.5	.0100	4.34	450
BEAM T-1	4.5	.014	.0074	.030	4#6	3#5	#2	3.5	.0100	4.79	530
BEAM T-2	4.5	.014	.0074	.028	4#6	3#5	#2	3.5	.0100	4.61	462
BEAM T-3	4.5	.014	.0140	.028	4#6	4#6	#2	3.5	.0100	4.47	470

ℓ - length of cantilever
d - effective depth
ρ - top steel reinf. ratio
ρ' - bottom steel reinf. ratio
ρ'' - volume of ties/volume of bound concrete core
ρ_b - balanced steel ratio
f'_c - concrete cylinder strength
f_r - modulus of rupture of concrete
* - yield strength = 65.5 Ksi
** - yield strength = 66.5 Ksi
*** - yield strength = 60.0 Ksi

The reinforcement of these beams was designed in accordance with the seismic provisions of the ACI 318-71 Code [9]. The basic properties of these beams are shown in the table of specimen properties.

Experimental Set-Up. - The beams were loaded at the cantilever tip by means of a double-acting hydraulic jack. Extensive electronic instruments were used to record continuously the basic deformation parameters, such as local strains in the reinforcement, curvatures, shear distortions, as well as the displacements at the tip of the cantilever. Shear distortion was measured by a pair of clip gages mounted on the diagonally-opposite corner points of the critical region. Each of the two clip gages provided a measurement of the relative movement of two diagonally-oriented points. From these measurements, the average shear distortion, γ_{av}, can be obtained geometrically, Fig. 3, as $\gamma_{av} = (\Delta-\bar{\Delta})d/(\alpha bh)$.

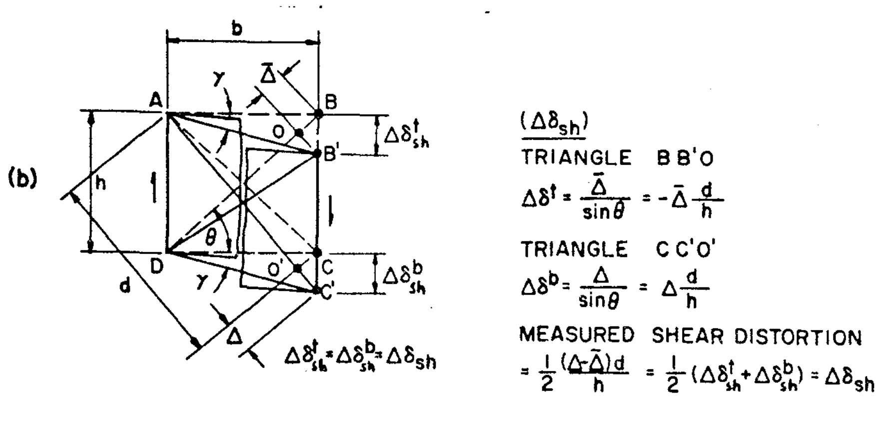

Fig. 3 Measurement of Shear Distortion

Due to γ_{av}, the change in the beam deflection is given by:

$$\delta_{sh} = \gamma_{av} b = (\Delta - \bar{\Delta}) d/(\alpha h) \tag{1}$$

For the photogrammatic study, one of the side surfaces of the critical region of the test beam at various loading stages was photographed on glass plates by a special camera mounted on a fixed stand. The photographed surface was subdivided into a fine grid to provide the necessary geometrical reference. To determine the change in geometry of the critical region, the position of the intersecting points of the grid lines and the opening of the cracks were read from the photo plates by a high precision comparator.

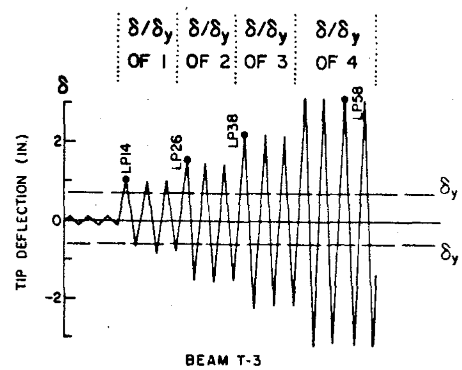

Fig. 4 Displacement Loading History

Loading Program. - Most test beams were subjected to a series of step-wise increasing symmetric displacement cycles. At each step, two to four cycles with the same displacement amplitude were made. This amplitude was increased so that the displacement ductility ratio, δ/δ_y, increased by one until failure or an instant when a significant drop in strength occurred. A typical tip deflection history is shown in Fig. 4. In addition, one specimen, R-4, was monotonically loaded to failure, and another, R-2, was subjected to unsymmetric displacement cycles.

GENERAL BEHAVIOR OF TEST BEAMS

Mechanism of Failure. - After flexural yielding, the failure of the unsymmetrically reinforced beams, ($\rho'/\rho < 1.0$), which were subjected to full reversals, was accelerated by local buckling of the bottom No. 5 bars near the fixed end of the beam during downward loadings. For the symmetrically reinforced beams, R-5 and R-6, failure appears to be due to the gradual loss of shear transfer capability along one or more cracks which crossed the whole beam section. These cracks developed during cyclic load reversals at a $\delta/\delta_y \geq 2$.

Inelastic Rotations. - The maximum inelastic rotation, θ_{PL}, at the initial position ranged from 0.026 rad. to 0.058 rad. The lowest value of θ_{PL} was obtained with the short beam, R-5; the highest value, with Beam R-4, which was subjected to a monotonically increasing load. The greater the shear span ratio, a/d, of the beam (i.e., the lower the magnitude of shear force during inelastic load reversals), the greater the energy dissipation capacity. For example, the maximum nominal shear stress induced during inelastic load was $3.5\sqrt{f'_c}$ in Beam R-6 (a/d = 4.46) and $5.3\sqrt{f'_c}$ in Beam R-5 (a/d = 2.75), reflecting an improvement in energy dissipation capacity by about 120%.

Shear Force - Shear Distortion Diagrams. - To study the effect of shear on the overall hysteretic behavior of a beam, the applied shear force, V, was plotted against the average angle of distortion, γ_{av}, measured in the region within 1.5 in. to 14 in., (i.e., approximately 1.0d) from the fixed end of the cantilever. A typical diagram is shown in Fig. 5. The repeated cycles in each load step are indicated by dashed lines and the first cycle by solid lines. Two main characteristics

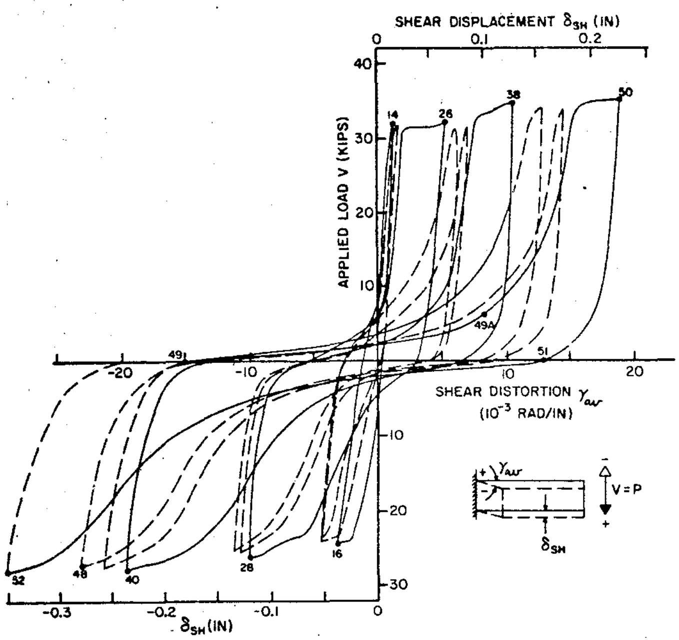

Fig. 5 V-γ_{av} Diagram (Beam T-3)

are depicted by these diagrams.

(1) During reloadings the loops exhibited a range of reduced stiffness at small loads. This occurred after a number of cyclic loadings in the inelastic range at a displacement ductility ratio of $\delta/\delta_y \geq 2$. This reduction in stiffness produced a noticeable pinching of the hysteretic loops. This behavior can be explained as follows.

During a cycle of load reversal, flexural and diagonal tension cracks occurred on both the top and bottom of the beam. Since the reinforcement was strained inelastically during loading, these cracks remained open after unloading. Upon reloading in the opposite direction, the shear was mostly resisted by the degrading aggregate interlocking and friction along the cracks and by the usually smaller dowel action of the main reinforcement. The stiffness of the beam increases again only when the cracks close because then the effectiveness of interlocking and friction increases and the composite action of the concrete and web reinforcement starts to resist shear. This mechanism of stiffness degradation was confirmed by the photogrammetric study of the incremental deformations in a typical inelastic half-cycle which is described later.

(2) When the specimens were cycled between fixed amounts of peak deflection, the degradation in shear stiffness of the critical region increased progressively from cycle to cycle as illustrated in Fig. 5. In other words, no stabilization of loops was achieved when cycles were repeated. This degradation becomes more pronounced as the applied deflections are increased and is due to the deterioration of the interface shear resistance at the cracks, tie resistance, and poorer dowel action. This is accentuated by the crack opening up through the whole beam cross-section during the repeated reverse loadings. Further discussion of this behavior is given later.

PHOTOGRAMMETRIC STUDY RESULTS

In a critical region of a R/C member subjected to severe reverse bending and shear, significant deformations are concentrated at the cracks. These deformations can be divided into shear deformation, $\Delta\delta_{crack}$, and flexural deformation, $\Delta\delta_{f\ crack}$. Both types of deformation are illustrated in Fig. 6. For a single crack, the quantity $\Delta\delta_{crack}$ represents a rigid body translation of piece B with respect to piece A, and $\Delta\delta_{f\ crack}$, a rotation of piece B with respect to A. If the crack remains open, the amount of shear deformation will be controlled by the following factors: (1) Stirrup elongation, which depends on the width of a crack and the effectiveness of stirrup anchorage; (2) Effectiveness of aggregate interlocking and friction resistance along the crack, which depends on the width of a crack; (3) Dowel

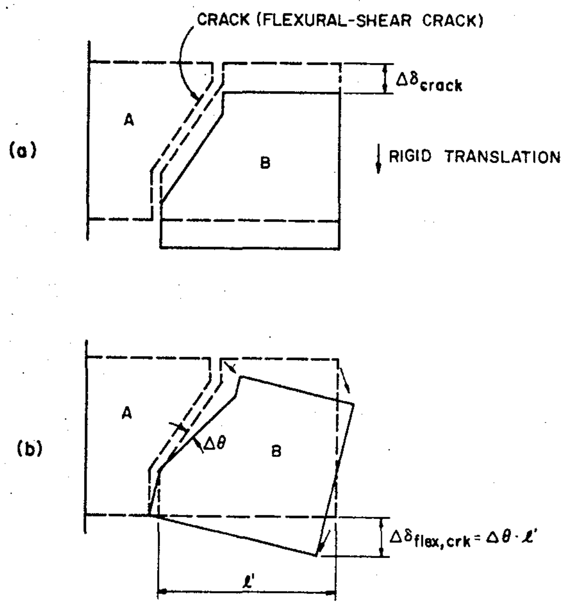

Fig. 6 Deformations at a Crack

deformation of longitudinal reinforcement, which strongly depends on the diameter of a bar, the width of a crack, and the spacing of the transverse reinforcement.

On the other hand, flexural deformation at the crack will be controlled by (1) Stresses developed in the longitudinal steel; (2) Width of the crack; (3) Effectiveness of the longitudinal reinforcement anchorage (bond); (4) Resistance offered by the ties at the inclined crack; and, (5) Condition of concrete in the compression zone, i.e., the degree of crushing or cracking.

The deformation pattern of the critical region of Beam T-3 during a half-cycle at $\delta/\delta_y = 4$ (load points 49-51, Fig. 5) is shown in Fig. 6. The displacements of the grid points are plotted on a larger scale than that for the reference grid. Two successive deformation fields are plotted in each figure to show the incremental changes in deformation. The deformation field corresponding to the previous load point is drawn in dashed lines and the subsequent one in solid lines.

LP 49 to LP 49A [0 kips to 6 kips, Fig.7(a)]- During this stage of the response the shear resistance is small and the amount of shear distortion is large. The deformation pattern of the critical region is distinctly translational, and the deformation caused by the the rotation of the beam is relatively small. The translational deformation is mainly due to the shear displacement across the cracks. One noticeably large shear displacement (0.1 in.) occurs at a vertical crack about 4 in. away from the support. At this stage of loading, the total beam deflection about 25.5 in. away from the beam support is 0.44 in.

LP 49A to LP 50 [From 6 kips to 35 kips, Fig.7(b)] - The incremental deformation pattern at this stage of the response is largely rotational. Although some rotation of the beam had already occurred from LP 49 to LP 49A, it was very small compared to the amount of shear deformation. As the loading continued beyond LP 49A, the cracks in the compression zone started to close under the increasing compression due to flexure. The increase in beam deflection, δ_{crit}, at 25.5 in. from the support is 1.25 in. The calculated deflection based on the average rotation of the vertical grid lines is 1.06 in. The difference between these values suggests that the magnitude of shear distortion was relatively small, i.e., 0.19 in.

LP 50 to LP 51 [From P = 35 kips to 0 kips, Fig.7(c)] - On release of load, the beam deflection is reduced. The incremental deformation taking place during unloading is primarily due to beam rotation. The amount of shear deformation is small compared to the shear deformation that occurred at the initial stage of the half-cycle (see also Fig. 5). The reason for this is that the cracks in the compression zone, which were closed at LP 50, stayed in contact during the unloading process. Hence, aggregate interlocking and friction were effective in restraining the shear distortion.

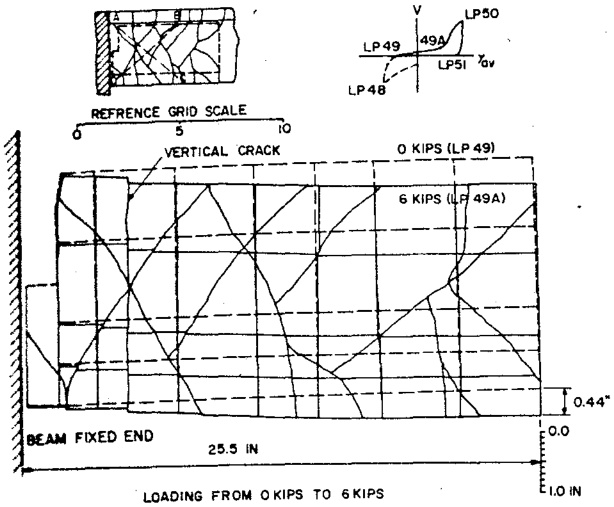

(a) LP's 49 - 49A

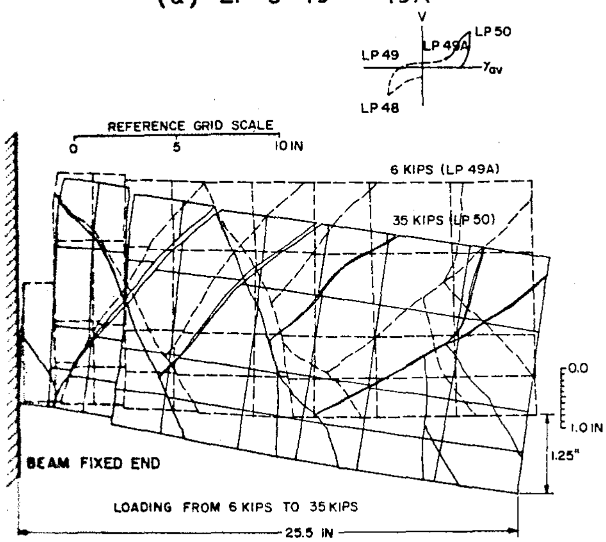

(b) LP's 49A - 50

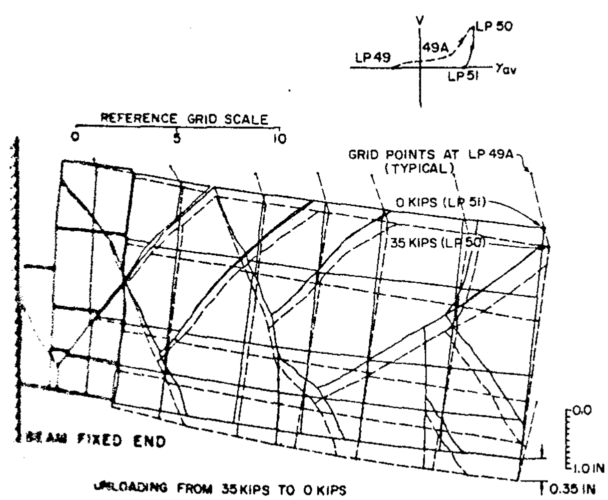

(c) LP's 50 - 51

Fig. 7 Photogrammetric Results (Beam T-3)

SHEAR DEGRADATION MECHANISMS

This mechanism is illustrated in Fig. 8. A brief discussion of its main stages follows.

Stage I (Initial Loading Stage)*. - After the beam has undergone one or more loading reversals, barely inducing yielding of the main reinforcement, some vertical and inclined cracks develop through the entire cross-section of the critical region due to residual tensile strain accumulated in the steel. Large shear deformations (relative translation movements) at these open cracks may lead to the progressive grinding of the concrete and the development of considerable dowel action. The development of dowel action usually leads to the splitting of concrete, causing bond deterioration along the main reinforcing bars. As a result, aggregate interlocking,friction and dowel action will become less effective as the number of reversals increases.

Stage II (Advanced Loading Stage. - At this stage, cracks in the compression zone are closed under increasing compression due to flexure. The shear force acting at the crack can cause progressive grinding of the concrete, resulting in a smooth contacting surface, and the resistance of aggregate interlocking and friction will become less effective as the number of reversals increases. The restraint offered by the stirrup-ties across the crack could become less effective due to degradation of the bond along their anchorage (embedment) lengths in the concrete beam.

As a result of high compression and lateral swelling of the concrete core, the concrete cover may crush and spall around the beam near the support. This would reduce the effectiveness of the compression zone to transfer shear. Only the

*The end of the initial loading stage is defined as the time when there is a distinct increase in shear stiffness, i.e., an increase in the slope of the shear force-shear distortion loading curve.

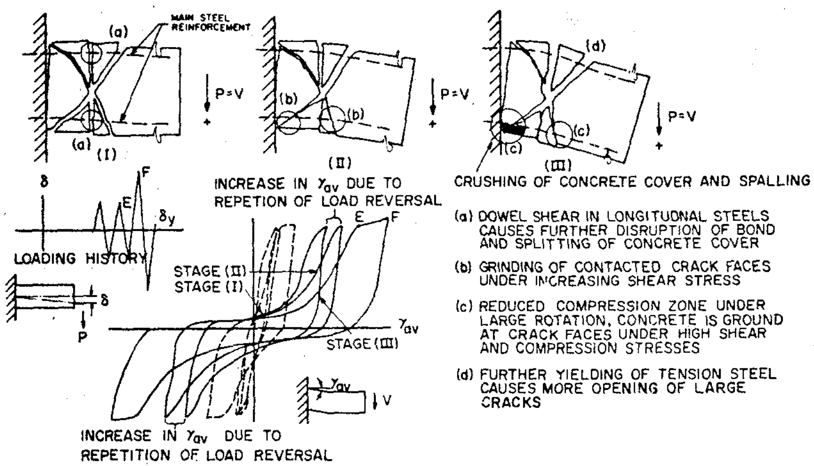

Fig. 8 Shear Degradation Mechanism

smaller zone of the confined core in compression would remain effective. Therefore the computation of the ultimate nominal shear stress recommended by the ACI Code [9], wherein $v_u = V_u/bd$, cannot be applied at this stage unless it is modified by replacing b,d of the gross section area by those of the confined core.

Stage III (Unloading Stage). - Upon the release of external loads, the deformations in the critical region are reduced. However, the change in deformation during this unloading is usually smaller than that which occurs during loading. It is unlikely that any significant shear degradation could occur during unloading.

The damages that occur during Loading Stages I and II accumulate and cause an increase in shear distortion with each repetition of a loading reversal.

Shear Degradation Due to An Increase in Applied Beam Displacement. - As the magnitude of the applied peak tip beam displacement, δ, increases during inelastic loading reversals, the moment carried by the beam will usually increase (at least up to a certain value of δ) due to strain-hardening of the main reinforcement. This, in turn, causes the yielding of the main reinforcement to spread further along the beam, thereby increasing the length of the critical region. Furthermore, the existing cracks open up more, resulting in greater shear distortion at the cracks. The increase in shear distortion due to an increase in peak beam displacement is indicated by line E F of the diagram in Fig. 8.

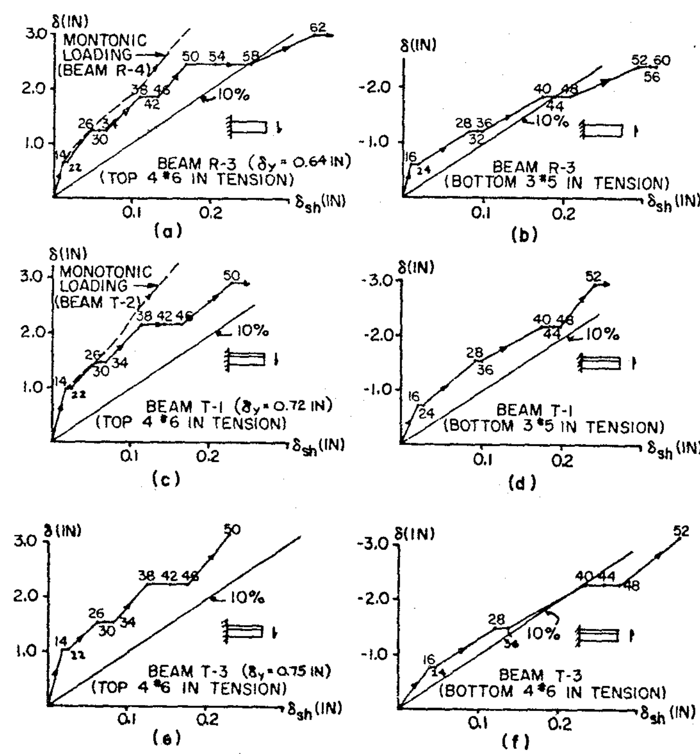

Fig. 9 Magnitude of δ_{sh} vs. δ

SHEAR DISTORTION RESPONSE OF TEST BEAMS

To study the effects of the different parameters on the shear behavior of the test beams, the peak shear distortion for each inelastic loading cycle is plotted against the tip deflection of the

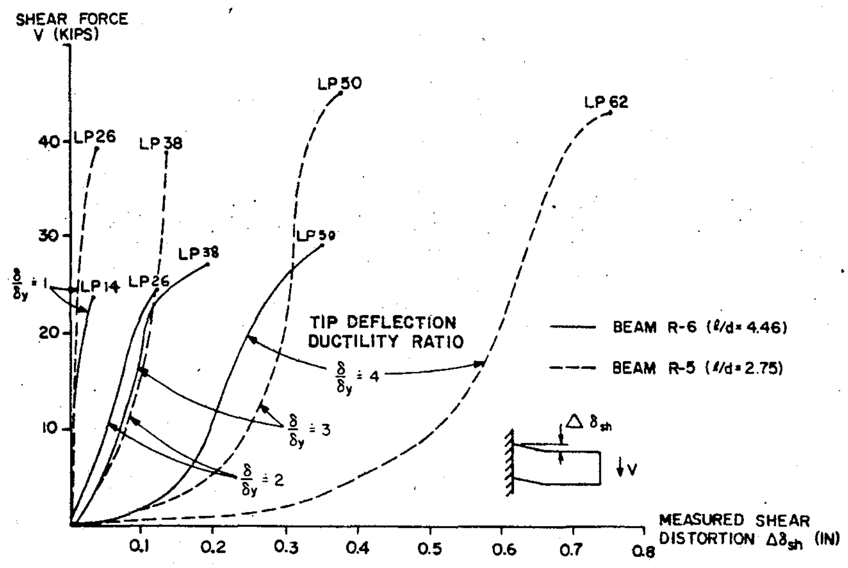

Fig. 10 Comparison between V - $\Delta\delta_{sh}$ Response of Beams R-6 and R-5

beam (Fig. 9). The shear distortion versus tip deflection points in the same loading sense are connected by straight lines; thus, the history of change in shear distortion from cycle to cycle can be easily observed.

Effect of Loading Sequence. - A comparison between monotonic and cyclic loading curves shows that under cyclic loading, shear distortion tends to increase with each repeated cycle of inelastic load reversal, i.e., from LP 26 to LP 34, and from LP 38 to LP 46, Figs. 9(a) and 9(c). This effect causes more shear to occur in cyclically loaded beams.

Effect of Relative Amount of Top and Bottom Steel Reinforcement. - This effect can be seen by comparing the results of similar beams, Beams T-1 and T-3, with the same amount of top reinforcement but with different amounts of bottom reinforcement (see Fig. 2). The results are comparable at the same load point number having similar beam displacement ductility values. The results indicate that the larger amount of steel at the bottom of Beam T-3 caused more shear distortion to occur in the peak upward load points, i.e., LP's 28 to 52 in Fig. 9(f) and 9(d), respectively. At the peak downward loadings, the amount of shear distortion reached by the two beams are similar, i.e., at LP's 14 to 50 in Figs. 9(e) and 9(c) respectively.

Effect of Slab in T-Beam. - The effect of slab on shear distortion can be seen by comparing results for Beams T-1 and R-3. The results indicate that the value of shear distortion occurring in Beam T-1 in the downward direction is larger than that in Beam R-3. This is due to a larger amount of shear force which developed in the downward loading direction in Beam T-1, because the slab reinforcement in Beam T-1 increases the downward moment capacity and the shear force acting in that direction.

Effect of High Shear Force. - Beams R-6 and R-5 were symmetrically reinforced but had different spans (38.5 in. vs. 62.5 in.). The maximum nominal shear stress developed in Beam R-6 was about 34% less than that in Beam R-5. The effect of high shear can be seen by comparing the shear force-shear distortion loading curves of the two beams at comparable ductilities, as shown in Fig. 10. The curves are shifted to the same origin for ease of comparison. As the deflection ductility of the loading reversals increased, there was increasingly more degradation in shearing stiffness in Beam R-5 during the initial loading stages, and there also was a greater amount of shear distortion at comparable cycles.

CONCLUSIONS

1. Beams subjected to severe shear reversals develop cracks across their entire section. Therefore, the shear should be resisted by web reinforcement, dowel action, aggregate interlocking, and friction at the cracks, rather than concrete. The latter resistance becomes less effective as the crack widths increase, causing large shear distortion which contributes to the deflection of a beam. Yielding of the main reinforcement must occur simultaneously, thereby widening the cracks. This is a combined flexure-shear degradation mechanism.

2. Hysteretic behavior of beams subjected to shear reversals inducing the same displacement shows significant degradation with the increasing number of cycles. The degree of degradation increases as the magnitude of shear increases.

3. Photogrammetric study of a half-cycle of a beam at a deflection ductility of four indicates that during the initial loading stage the deformation pattern in the critical region is essentially translational. This is due to the shear deformation at those cracks which remain open throughout the entire beam section.

4. The possible shear degradation mechanisms are (1) the opening of cracks due to yielding or slippage of main reinforcement; (2) the spalling of the concrete cover around the periphery of the flexural critical region; (3) the tie deformation across the cracks due to increase in the degradation in stirrup-tie anchorage; (4) the crushing and grinding of concrete at the crack surfaces which can lead to less effective aggregate interlocking along the cracks; and (5) the local disruption of bond between the longitudinal steel and concrete due to the shear forces developed at the steel by its dowel action along the open cracks.

IMPLICATIONS TO SEISMIC DESIGN

In the ultimate strength design, as well as in the seismic design of R/C members, it is essential to provide enough shear capacity in possible hinge locations to develop flexural strength. In aseismic design, it is important to assure that such regions will not fail in shear before adequate rotation is developed at a nearly constant maximum moment and that the effect of pinching of the hysteretic loops due to shear degradation on the energy dissipation capacity of the region is minimized. To reduce the potential shear degradation in the critical regions, it is necessary to develop good shear resistances along all the regions where large cracks might occur. The use of closely spaced stirrup-ties and supplementary ties has proven to be effective in improving the rotation and energy capacities of R/C flexural critical regions. This is so since not only more shear reinforcement is provided to prevent formation of the inclined cracks, but also because such reinforcement provides better confinement of concrete and acts as a more effective support for the longitudinal compression steel. In very short beams, however, a major crack traversing the whole section can develop between two adjacent vertical ties; consequently, these ties cannot function as shear reinforcement. In this case, the use of inclined reinforcing bars appears to be a practical solution [5].

ACKNOWLEDGEMENTS - This work was supported by the National Science Foundation, Grant No. AEN73-07732A02. The assistance with the experimental program of Dr. H. Krawinkler and graduate students, S. Viwathanatepa, D. Soleimani, P. Wong and T. Y. Wang is gratefully acknowledged.

REFERENCES

1. Bertero, V. V., "Experimental Studies Concerning Reinforced, Prestressed and Partially Prestressed Concrete Structures and their Elements," IABSE Symposium, Lisbon, 1973.

2. Brown, R. H., and Jirsa, James O., "Reinforced Concrete Beams under Load Reversals," ACI Journal, Vol. 68, No. 5, May 1971.

3. Park, R., Kent, D., and Sampson, R., "Reinforced Concrete Members with Cyclic Loading," Journal of the Structural Division, ASCE, Vol. 98, No. ST7, July 1972.

4. Popov, E. P., Bertero, V. V., and Krawinkler, H., "Cyclic Behavior of Three R.C. Flexural Members with High Shear," EERC Report No. 72-5, University of California, Berkeley, October 1972.

5. Bertero, V. V., Popov, E. P., and Wang, T. Y., "Hysteretic Behavior of Reinforced Concrete Flexural Members with Special Web Reinforcement," EERC Report No. 74-9, University of California, Berkeley, August 1974.

6. Krawinkler, H., and Popov, E. P., "Hysteretic Behavior of Reinforced Concrete Rectangular and T-Beams," Proceedings, 5WCEE, Paper 28, June 1973, Rome.

7. Bertero, V. V., and Popov, E. P., "Seismic Behavior of Ductile Moment-Resisting R/C Frames," ACI, (in press).

8. Ma, S. M., Bertero, V. V., and Popov, E. P., "Hysteretic Behavior of Reinforced Concrete Rectangular and T-Beams," EERC Report, University of California, Berkeley, (in press).

9. ACI Standard Building Code Requirements for Reinforced Concrete (ACI 318-71), American Concrete Institute, Detroit, Michigan 1971.

50272-101

REPORT DOCUMENTATION PAGE	1. REPORT NO. NSF/RA-760837	2.	3. Recipient's Accession No.

4. Title and Subtitle
Cyclic Shear Behavior of R/C Plastic Hinges *

5. Report Date
March 31, 1976

6.

7. Author(s)
S.Y.M. Ma, and E.P. Popov

8. Performing Organization Rept. No.

9. Performing Organization Name and Address
University of California at Berkeley
Department of Civil Engineering
Berkeley, California 94720

10. Project/Task/Work Unit No.

11. Contract(C) or Grant(G) No.
(C)
(G) AEN7604263

12. Sponsoring Organization Name and Address
Applied Science and Research Applications (ASRA)
National Science Foundation
1800 G Street, N.W.
Washington, DC 20550

13. Type of Report & Period Covered

14.

15. Supplementary Notes
*Partial proceedings of American Society of Civil Engineers, Engineering Mechanics Division Specialty Conference, University of California at Los Angeles, March 30-31, 1976

16. Abstract (Limit: 200 words)
Results are presented of an attempt to define the actual mechanisms of degradation in stiffness, strength and energy capacities that have been observed in the critical regions under earthquake-like excitations. The main data analyzed were obtained from tests on nine cantilever beams. After a brief description of the test specimens and test procedures, the general behavior of the beams is discussed, with emphasis on the failure mechanism and how it is modified under different amounts of shear. Conclusions regarding the observed behavior are drawn, and their implications in aseismic design of ductile resisting frames are discussed. It is noted as essential to provide enough shear capacity in possible hinge locations to develop flexural strength. To reduce the potential shear degradation in the critical regions, it is necessary to develop good shear resistances along all the regions where large cracks might occur. The use of closely spaced stirrup-ties and supplementary ties has proven to be effective in improving the rotation and energy capacities of R/C flexural critical regions. In very short beams, however, a major crack traversing the whole section can develop between two adjacent vertical ties. Consequently, these ties cannot function as shear reinforcement. In this case, the use of inclined reinforcing bars appears to be a practical solution.

17. Document Analysis a. Descriptors

Earthquake resistant structures	Shear properties	Seismic waves
Dynamic structural analysis	Reinforced concrete	Flexural strength

b. Identifiers/Open-Ended Terms

Reinforced concrete (R/C)

c. COSATI Field/Group

18. Availability Statement	19. Security Class (This Report)	21. No. of Pages
NTIS		13
	20. Security Class (This Page)	22. Price A02 - A01

(See ANSI–Z39.18) See Instructions on Reverse

OPTIONAL FORM 272 (4–77)
(Formerly NTIS–35)
Department of Commerce